Computational Study of the Adsorption of Dimethyl Methylphosphonate (DMMP) on the (010) Surface of Anatase TiO$_2$ With and Without Faceting

V.M. Bermudez*

Electronics Science and Technology Division

Naval Research Laboratory

Washington, DC 20375

* Phone: +1-202-767-6728

 FAX: +1-202-767-1165

 victor.bermudez@nrl.navy.mil

Report Documentation Page

1. REPORT DATE **05 DEC 2009**	2. REPORT TYPE	3. DATES COVERED **00-00-2009 to 00-00-2009**

4. TITLE AND SUBTITLE **Computational Study of the Adsorption of Dimethyl Methylphosphonate (DMMP) on the (010) Surface of Anatase TiO2 With and Without Faceting**	5a. CONTRACT NUMBER
	5b. GRANT NUMBER
	5c. PROGRAM ELEMENT NUMBER
6. AUTHOR(S)	5d. PROJECT NUMBER
	5e. TASK NUMBER
	5f. WORK UNIT NUMBER

7. PERFORMING ORGANIZATION NAME(S) AND ADDRESS(ES) **Electronics Science and Technology Division,Naval Research Laboratory,Washington,DC,20375**	8. PERFORMING ORGANIZATION REPORT NUMBER

9. SPONSORING/MONITORING AGENCY NAME(S) AND ADDRESS(ES)	10. SPONSOR/MONITOR'S ACRONYM(S)
	11. SPONSOR/MONITOR'S REPORT NUMBER(S)

12. DISTRIBUTION/AVAILABILITY STATEMENT
Approved for public release; distribution unlimited

13. SUPPLEMENTARY NOTES

14. ABSTRACT

15. SUBJECT TERMS

16. SECURITY CLASSIFICATION OF:			17. LIMITATION OF ABSTRACT	18. NUMBER OF PAGES	19a. NAME OF RESPONSIBLE PERSON
a. REPORT **unclassified**	b. ABSTRACT **unclassified**	c. THIS PAGE **unclassified**	**Same as Report (SAR)**	**29**	

Abstract

The adsorption of dimethyl methylphosphonate (DMMP) on the (010) surface of anatase TiO_2, which is isostructural with the (100), has been studied using density functional theory and two-dimensionally-periodic slab models. The experimentally-observed faceting of this surface has, for the first time, been included in the modeling. The relaxations of bare surfaces both with and without faceting are similar, leading to an atomic-scale roughening due to inward (outward) displacement of five-fold-coordinated Ti_{5c} (six-fold-coordinated T_{6c}) atoms together with outward displacement of three-fold-coordinated O_{3c} atoms. Molecular adsorption occurs by formation of a Ti_{5c}---O=P dative bond with one or more C-H---O_{2c} bonds between CH_3 groups and unsaturated, two-fold-coordinated (O_{2c}) sites. The energies for molecular adsorption, obtained using the B3LYP functional, are virtually identical (about -21.0 kcal/mol) for the two surfaces and are also close to those found elsewhere for the rutile (110) and anatase (101) surfaces. A possible first step in the dissociative adsorption of DMMP has also been modeled and is found to be thermodynamically favored over molecular adsorption to a degree which depends on faceting.

1. Introduction

The surface structure and properties of TiO_2, in both the rutile and anatase forms, have been intensively studied both experimentally and computationally [1]. For either form, the adsorption of a wide variety of molecules has been investigated on several different crystallographic planes. An especially important aspect is adsorption on the isostructural (100) and (010) surfaces of anatase[1]. Many of the technological applications for TiO_2, in which the material is used as a catalyst, a photocatalyst [2] or a catalyst support, involve high-surface-area (HSA) powders prepared by burning $TiCl_4$ in O_2. The Degussa P25 powder, which has been widely used in surface-chemistry experiments on TiO_2, is an example of such material. Typically these powders are ~80% anatase, and experiment [3-5] shows that in this case the (010) is the dominant surface. The (100) is also known to make a major contribution to the surface area of anatase nanocrystals [6] and to be especially active in photocatalysis [7]. Recent work by Dzwigaj et al. [8] has clearly shown that the morphology of anatase powder (i.e., the distribution of exposed crystal planes) depends on the method of fabrication and treatment. However, in general the (100) surface appears to have a significant, if not always dominant, presence in many forms of anatase powder.

Experimental data for this surface are scarce, due to the difficulty in obtaining anatase samples suitable for single-crystal studies. However, several computational studies of adsorption have been reported, focusing on atomic H [9-11], NH_3 and NO [12], CO_2 [13], H_2O [12,14], O_2 [14], chlorobenzene [15], chlorophenol [16], N heterocycles [17], acetic acid [18] and oxalic acid [19]. In most cases unsaturated, five-fold-coordinated (Ti_{5c}) sites are active as Lewis-acid adsorption sites. In particular the adsorption behavior of the bidentate reagent oxalic acid on ana-

---

[1] The designations (100) and (010) will be used interchangeably since the two anatase surfaces are isostructural, as are the (101) and (011). Some of the literature on anatase powder refers to the (010), and that labeling is used here except, in the Introduction, when citing works which refer explicitly to (100).

tase (100) differs from that on rutile (110) due the differing local arrangement of Ti_{5c} surface sites [19]. Unsaturated, two-fold-coordinated (O_{2c}) sites can also be involved in hydrogen bond (H-bond) formation. The effects, on the structure of the (100) and other anatase surfaces, of hydroxylation and of steady-state ambient pressures of H_2, H_2O and H_2S have been thoroughly investigated in a series of density functional theory (DFT) studies by Arrouvel et al. [20,21]. These studies have provided important insight into the properties of real TiO_2 catalysts.

Figure 1 shows schematic models for the (010) surface which, except for the (101), has the lowest surface energy (σ) for anatase [20,22]. Figure 1a shows the ideally-terminated (unrelaxed) surface, and Fig. 1b shows the (1x2) faceted surface (also unrelaxed) observed [23] in scanning tunneling microscopy. Faceting of the (100) surface exposes the more stable (101), which is isostructural with the (011). Computation [20,22] shows $\sigma = 0.44$ and 0.53 J/m^2 for the relaxed (101) and (100) surfaces, respectively, *vs.* 0.31 J/m^2 for rutile (110). The effect of faceting on the anatase (100) σ is unknown at present. All (100) surface Ti sites are Ti_{5c} while half the surface O atoms are O_{2c} and half are saturated, three-fold-coordinated O_{3c} sites. With equal numbers of singly-unsaturated Ti_{5c} and O_{2c} sites the surface is auto-compensated, meaning that the excess electron density on a Ti_{5c} is transferred to an O_{2c} to maintain a closed-shell configuration on both. Hence, there is no indication [10,17] of surface states in the band gap of the relaxed but unfaceted surface. Adsorption on the faceted surface, which has not to our knowledge been studied previously, should be especially interesting. For an appropriately-chosen molecule the structure of this surface, with rows of Ti_{5c} sites set below and in close proximity to rows of O_{2c} sites, holds out the possibility of both dative bonding to a Ti_{5c} and H-bonding to multiple O_{2c} sites.

The purpose of this work is to examine the adsorption of a fairly complex molecule, $(CH_3O)_2(CH_3)P=O$ (dimethyl methylphosphonate, DMMP), on the anatase (010) surface both

with and without faceting. This is, to our knowledge, the first computational study of the faceted anatase (010) surface with or without adsorbates. Our interest in DMMP stems from the use of this species as a simulant for chemical warfare agents (CWAs) such as Sarin and the demonstrated utility of TiO_2 in the catalytic destructions of CWAs (refs. 24-28 and works cited). The growing interest in HSA TiO_2 powders for this application, and the wide-spread use of DMMP in experimental work relating to CWAs, makes such a study timely. For two reasons, the present work focuses on adsorption of DMMP on bare surfaces, free of defects or co-adsorbed species. Firstly, the adsorption of DMMP on TiO_2, even under these ideal conditions, remains controversial. Secondly, the experimental data for this system [29-32] with which we will compare our results were all obtained in vacuum or in ultra-high vacuum (UHV).

2. Computational and modeling details

2.1 Geometry optimization and energy calculations

All calculations were done using two-dimensionally-periodic slab (2-DPS) models and the *CRYSTAL 06* code [33-35] which employs Bloch functions constructed from localized Gaussian basis sets. To reduce the computational cost, geometry optimization was done at the restricted Hartree Fock (RHF) level. This has previously been shown [36,37] to give results for the bulk and surface structures of TiO_2 which are very close to those obtained using DFT. Optimization at the RHF level has also been shown to give reliable results for molecular geometries [38]. For Ti, the Hay-Wadt small-core effective-core pseudopotential (ECP) was used with the 411(311d)G basis set previously optimized for perovskite titanates [33,39]. For O, a 6-31G(d) all-electron basis set [40] was used with the exponents of the outermost shells re-optimized[2] for bulk rutile. The optimized parameters were 0.27281 and 0.31201 Bohr^{-2}, respectively, for the *sp* and *d* shells. The

---

[2] Basis-set optimization was done using *CRYSTAL 03* with the *LoptCG* script (C. Zicovich-Wilson; Universidad Autonoma del Estado de Morelos; Cuernavaca, Mexico).

bulk lattice constants and atom positions optimized using this procedure show good agreement with experiment (Table 1). In subsequent geometry optimizations, the lattice constants were fixed at these values while the positions of all Ti and O atoms (as well as those of the DMMP atoms) were allowed to vary. For DMMP, 6-31G(d,p) basis sets from a standard database [40] were used without modification.

After geometry optimization, a single-point calculation of the total energy was done using DFT with all-electron basis sets and the B3LYP functional, which has been shown [37,41] to give reliable results for the bare surfaces of both rutile and anatase. A discussion of the use of B3LYP in describing the adsorption of DMMP is given elsewhere [42]. For TiO_2 the basis sets are designated 86-411(d31)G for Ti and 8-411d1G for O, while the 6-31G(d,p) basis sets were again used for DMMP. For Ti and O the outermost *sp* and *d* shells have been optimized [41] for TiO_2, and the complete basis sets are obtained by combining these with the inner shells given elsewhere [33]. Preliminary calculations using somewhat larger 6-311G(d,p) basis sets [40] for DMMP led to difficulties in converging the self-consistent field (SCF). This may result from the small exponent in the outermost *sp* shell of the P atom (0.0684930 Bohr^{-2}) which can cause linear-dependency problems in calculations for periodic structures [33].

The bulk calculations used an (8x8x4) sampling grid, giving a k-point spacing of ~0.1 atomic units (au). Calculations for the (4x1) and (4x2) supercells used in adsorption (see Sec. 2.2) were done with (1x2) and (1x1) grids respectively, giving a k-point spacing of ~0.2 au. Reducing the k-point spacing to 0.1 au for the (4x1) supercell had a negligible effect on the energy. Following Labat et al. [37], an "extra-large" (75,974) integration grid was used for all DFT calculations. In *CRYSTAL*, truncation of the sums of Coulomb and exchange terms in the Fock matrix is determined by five overlap criteria [33,35] (T1–T5). These were set at 10^{-8} for T1–T4 and 10^{-18}

for T5. A high numerical accuracy in integration is generally required for TiO_2 [37,41] and is further necessitated by the small exponent (0.09983 Bohr^{-2}) in the outermost *sp*-shell of the P 6-31G(d) basis set. In the multipolar expansion zone [33-35] a maximum order of L= 6 was used. The geometry convergence criteria were 1×10^{-5} Hartree for energy, 1.8×10^{-3} Bohr for maximum displacement and 4.5×10^{-4} Hartree/Bohr for maximum gradient.

2.2 TiO$_2$ model structures

The 2-DPS model for the unfaceted surface used a (4x1) supercell with six layers, giving 48 TiO_2 units per cell. The lateral dimensions were chosen to give a low coverage of adsorbed DMMP (thus avoiding intermolecular interaction) while still being computationally affordable. The surface area of the supercell, containing one adsorbed DMMP, was 15.13 Å x 9.54 Å = 144.2 Å^2, and the coverage was 1/8-monolayer (one DMMP per eight surface Ti_{5c} sites). A slab thickness of six layers has been shown [22,37] to be adequate for convergence of the surface energy of anatase (100). For the faceted surface the supercell was increased to (4x2) in order to accommodate the facet. After removal of the appropriate atoms (cf. Fig. 1), the supercell comprised 80 TiO_2 units. In forming the facet, equivalent atoms on either side of the slab were removed so as to maintain inversion symmetry. Complete relaxation of the faceted surface will be seen (Sec. 3.1) to require a thicker slab. Thus calculations for the bare faceted surface were also done, for comparison, for a thickness of twelve layers and a (1x2) supercell. Since localized, rather than plane-wave, basis sets are used one can study an isolated 2-DPS. Hence the issue of the vacuum gap between slabs periodically repeated in the surface-normal direction does not arise.

A single DMMP molecule was placed on the "top" surface of the 2-DPS supercell, and a second was placed symmetrically on the "bottom" surface. This "two-sided" approach preserves the center of symmetry of the supercell, thus avoiding the production of a dipole potential, and

has been shown [43] to be beneficial in 2-DPS studies of H_2O adsorption on rutile (110). The adsorption energy per DMMP is then defined as

$$\Delta E_{ads} = [E(TiO_2+nDMMP) - E(TiO_2) - nE(DMMP) + \Delta E(BSSE)]/n$$

where $n = 2$, $E(TiO_2+nDMMP)$ is the relaxed total DFT energy with adsorbed DMMP, $E(TiO_2)$ and $E(DMMP)$ are the energies of bare TiO_2 and free DMMP and $\Delta E(BSSE)$ is the counterpoise correction for basis set superposition error. Thus $\Delta E_{ads} < 0$ indicates an exothermic process. All technical parameters (integration accuracy, etc.) were the same for all quantities to be combined in obtaining ΔE_{ads}. Specifically, $E(DMMP)$ was obtained in the same manner as the other energy terms; namely, by optimizing the geometry at the RHF/6-31G(d,p) level followed by a single-point B3LYP/6-31G(d,p) calculation. The free DMMP molecule was placed in the lowest-energy gas-phase conformation [44,45] before starting the optimization process.

3. Results

3.1 Relaxation of the bare surfaces

Table 1 shows the lattice parameters obtained in the present RHF calculation for bulk anatase and, for comparison, bulk rutile. In both cases, the agreement with experiment [46] is seen to be quite good. Table 2 shows the relaxation-induced displacements of atoms on and near the bare unfaceted surface in comparison to previous RHF results [37] for a somewhat thicker slab, together with corresponding results [22] using DFT in the geometry relaxation. The agreement among the three sets of results is again quite good. The relaxation is essentially identical for all equivalent atoms in the present (4x1) cell, which indicates no tendency toward reconstruction. Figure 2 and Table 3 show corresponding results for the faceted surface, which are more complex. For the 2-DPS described above, with 6 layers before faceting, there are differences in the displacements of equivalent atoms having different positions in the [001] direction. For example,

8

the two Layer 1 Ti_{5c} sites should be equivalent (cf. Fig. 1b) but exhibit somewhat different displacements during relaxation. However, equivalent atoms at different positions in the [100] direction have essentially identical relaxations.

These anomalies result from the fact that a thickness of only 6 layers is insufficient for complete relaxation when the slab is thinned by faceting. This is shown by results for a slab with 12 layers before faceting and a (1x2) supercell. Reducing the cell dimension in the [100] direction is permissible in view of the results obtained for the 6-layer slab. For the thicker slab the displacements of equivalent atoms are now essentially identical, but these are, in most cases, not very different from those for the thinner slab. The signs given for Δx in Table 3 are significant. Thus $O_{\perp}(1)$ and $O_{\perp}(2)$ in the Layer 1 displace away from the facet, and $O_{\perp}(1)$ and $O_{\perp}(2)$ in the Layer 2 displace away from the "channel". In Layer 6 of the 12-layer slab (not shown) the displacements from the bulk positions are all <0.03 Å in magnitude, indicating reasonably good convergence. Comparison of Figs. 1 and 2 shows that relaxation leads to an atomic-scale roughening of the surface, as noted previously [22,37], with $O_{\parallel}$ (Ti_{5c}) displacing outward (inward) along the surface normal. Finally, the density of states for either surface (not shown) revealed no surfaces states in the band gap, in agreement with previous results [10,17] for the relaxed unfaceted surface.

3.2 Molecular adsorption of DMMP

3.2.1 The unfaceted surface

Figure 3 shows the relaxed configuration of DMMP molecularly adsorbed on either surface. For the unfaceted surface (Fig. 3a) ΔE_{ads} = -21.0 kcal/mol was found after a BSSE correction of +6.5 kcal/mol. The Ti---OP and TiO=P bond lengths are 2.09 and 1.50 Å respectively, and the Ti---O=P bond angle is 138º. There appear to be two C-H---O_{2c} interactions that meet the H-bond criteria [47] for interatomic distances and angles. For Bond 1 (2) the H---O and C---O dis-

tances are 2.28 and 3.29 Å (2.65 and 3.67 Å) respectively, and the C-H---O angle in either case is 157°. Other possible C-H---O interactions (based on the H---O distances) involve much smaller angles generally indicative of a weaker bond. It is noted that ΔE_{ads} for the (010) surface is close to 2-DPS results obtained elsewhere [42] for molecular adsorption of DMMP on the anatase (101) and rutile (110) surfaces (-19.1 and -17.6 kcal/mol, respectively). The small variation in ΔE_{ads} reflects the trend in surface energies given above, with ΔE_{ads} decreasing in magnitude with increasing surface stability. On all surfaces, adsorption reverses the inward displacement of the Ti_{5c} bonding site that occurs when the bare, ideally-terminated surface relaxes. This can be seen clearly in Fig. 3a as an outward displacement of the Ti_{5c} adsorption site relative to the neighboring Ti_{5c} sites.

Other configurations, differing from that in Fig. 3a by rotation of the DMMP by 90° or 180° about the P=O bond, were also considered as starting points in the geometry optimization. These differ as to which combinations of CH_3 groups are positioned favorably for C-H---O_{2c} bond formation. At the RHF level used in geometry optimization the 90° (180°) rotations relaxed to energies which were higher by about 2.3 (9.0) kcal/mol than that of Fig. 3a. Another starting geometry, differing from that in Fig. 3a by a rotation of the DMMP by 180° about the Ti---OP bond, was also considered. This structure makes use of the slightly more distant O_{2c} sites for possible H-bonding. However, the relaxed structure was less stable by ~15 kcal/mol at the RHF level. Still other rotations, by 90° about the Ti---OP bond or by 180° about both the P=O and Ti---OP bonds also relaxed to structures which were unstable relative to that in Fig. 3a.

The fact that none of these starting structures relaxed to the apparently most stable configuration (Fig. 3a), but instead remained in approximately the initial conformation, indicates that there is a significant barrier to the bond rotations needed to accomplish the transformation. This

may arise from the need to break one or more C-H---O_{2c} bonds in order to accomplish the rearrangement. The existence of this barrier made it necessary to consider several different initial structures in the geometry optimization.

Finally, dative bonding between a Ti_{5c} and a methoxy O atom is also a possible mode of adsorption. This has been considered elsewhere [42] for the rutile (110) surface and been found to give a negligible ΔE_{ads}. In the present case, an attempt was made to adsorb DMMP on the unfaceted surface *via* a Ti_{5c}---O bond to a methoxy O atom. At the RHF level used in geometry optimization the resulting structure was less stable than that in Fig. 3a by ~25 kcal/mol, indicating an unstable configuration. Likewise, an initial structure with a Ti_{5c}---O=P bond together with a Ti_{5c}---O bond to a methoxy at an adjacent Ti_{5c} site relaxed to one with only the Ti_{5c}---O=P bond.

3.2.2 The faceted surface

For the faceted surface (Fig. 3b), DMMP was placed symmetrically on both slab faces at the $Ti_{5c}(1)$ site of Layer 2 shown in Fig. 2. The slab at this point is four layers thick, which should suffice for a nearly-converged ΔE_{ads}, and is preferable to the Layer 2 $Ti_{5c}(2)$ site where the slab is five layers thick. Previous work on the adsorption of CO [48] or H_2O [49,50] on rutile (110) shows that a thin 2-DPS with an even (odd) number of Ti layers tends to slightly underestimate (significantly overestimate) the fully-converged magnitude of ΔE_{ads}. Similar odd/even oscillations in the (100) surface energy are seen for thin anatase 2-DPS slabs [37].

For the faceted surface, $\Delta E_{ads} = -21.3$ kcal/mol was found using the same $\Delta E(BSSE)$ as above. The Ti---OP and TiO=P bond lengths are 2.04 and 1.49 Å respectively, and the Ti---O=P angle is 140º. All results are close to those given above for adsorption on the unfaceted surface. The dashed line indicates one of several possible H-bonding interactions, based on the H---O distances which are in the range of 2.39 to 3.00 Å. The indicated bond is believed to be the strong-

est, with O---H and C---O distances of 2.39 and 3.29 Å respectively and a C-H---O angle of 140º. Other interactions have smaller C-H---O angles and/or longer H---O distances and are therefore probably weaker [47]. It is possible, however, that the cumulative effect of several weak H-bonds might make a significant contribution to the total ΔE_{ads}. A quantitative discussion of H-bonding requires the characterization of bond critical points using the Atoms in Molecules theory [51] which is not available at present.

Alternative starting structures, differing from that in Fig. 3b by rotations of 70 or 140º about the P=O bond, were also considered in order to position various CH_3 groups for possible H-bonding to O_{2c} sites in Layers 1 and 2. However, these were less stable by about 3.5 and 7.2 kcal/mol respectively at the RHF level used in geometry optimization. As in the case of the unfaceted surface, neither of these initial structures relaxed to the most stable configuration during geometry optimization which suggests a significant barrier to the necessary bond rotation. Large rotations about the Ti---OP bond were also considered but were hindered by steric interactions between the CH_3O groups and the "step edge" between Layers 1 and 2.

As noted above, both Ti_{5c} sites in Layer 2 (Fig. 2) are equivalent on the semi-infinite surface but can differ for a thin 2-DPS. Adsorption at the $Ti_{5c}(2)$ site of Layer 2 was evaluated for DMMP in the same configuration as at the $Ti_{5c}(1)$ shown in Fig 3b. The bond lengths and angles in the relaxed structure, including those of the putative dominant H-bond, were virtually identical to those found for adsorption at $Ti_{5c}(1)$, but ΔE_{ads} was larger in magnitude by ~4.3 kcal/mol at the RHF level used in geometry optimization. On the basis of the above discussion, this is assumed to represent an overestimate. Adsorption outside the facet (i.e., at a Layer 1 Ti_{5c} site in Fig. 3b) was compared with adsorption inside the facet (i.e., at the Layer 2 Ti_{5c} site as shown in Fig. 3b). The starting geometry was the same as those identified above as the most favorable and

shown in Figs. 3a,b. At the RHF level the resulting ΔE_{ads} was 3.9 Kcal/mol smaller in magnitude than for adsorption inside the facet. The overall conclusion is that the results do not depend greatly on the choice of adsorption site but that the structure in Fig. 3b is the most favorable for molecular adsorption on the faceted surface.

3.3 Dissociative adsorption of DMMP

Figure 4 shows models for a possible first step in the dissociation of DMMP on surfaces with and without faceting. The structure is obtained by breaking a PO-CH$_3$ bond, moving the CH$_3$ to an O$_{2c}$ site and then forming a (CH$_3$)(CH$_3$O)P(-O-)$_2$ bridge between two Ti$_{5c}$ sites. This is only a formal description and is not intended to represent the actual reaction mechanism. The end product is consistent with the results of x-ray photoemission spectroscopy (XPS) and tempera-ture-programmed desorption (TPD) experiments for DMMP adsorbed at room temperature on OH-free single-crystal rutile (110) surfaces prepared and maintained in UHV [29,30]. These data show mainly molecular adsorption. The relatively small amount of decomposition that does oc-cur leads to the desorption of CH$_3$, but not CH$_3$O, in TPD. The yield of CH$_3$ is distinct from the cracking of desorbed DMMP itself and is consistent with CH$_3$ adsorbed at a bridging O$_{2c}$ site as opposed to a terminal CH$_3$-O-Ti site. Desorption of CH$_3$O from such a terminal site would re-form a Ti$_{5c}$; whereas, desorption of CH$_3$ would yield an unstable, doubly-unsaturated O atom un-less a Ti$_{5c}$ site were available for forming an O$_{2c}$ bridge. However, these data were obtained for rutile (110) and might not necessarily apply directly to anatase (010).

A thorough examination of all *a priori* possible dissociation products was not performed since the goal here is to determine the extent to which faceting affects dissociation, and the rela-tive energies for molecular *vs.* dissociative adsorption for a plausible structure. Several other dis-sociation structures are considered elsewhere [42] for DMMP on rutile (110) and anatase (101).

13

The starting configuration was based on the most-favorable structures for molecular adsorption discussed above and shown in Fig. 3. For the unfaceted surface, one alternative structure was considered in which the CH_3 was placed on one of the two equivalent O_{2c} sites which are closest to the bridge (i.e., one step to the right of that occupied in Fig. 4b). This alternative site is marked by an arrow in Fig. 4b. The OCH_3 on the bridge was also rotated 90° about the $P-OCH_3$ bond so as to move the CH_3 away from the $O_{2c}-CH_3$, thus minimizing steric repulsion between the two CH_3 groups and allowing C-H---O bonding between the $O_{2c}-CH_3$ and the O atom in the $P-O-CH_3$ group. At the RHF level the geometry-optimized ΔE_{ads} was negligibly different from (~1 kcal/mol larger than) that for the structure in Fig. 4b.

The BSSE-corrected ΔE_{ads} is -32.7 and -22.7 kcal/mol, respectively, for the unfaceted and for the faceted surface. These are larger than the energies given above for molecular adsorption but only slightly so for the faceted surface. This indicates that dissociation is thermodynamically favored to a degree which depends on faceting. As noted above, faceting exposes the more stable (011) surface, which is isostructural with the (101). Consistent with this, a 2-DPS calculation done elsewhere [42] for the dissociative adsorption of DMMP on the anatase (101) surface, in a structure like that studied here, gave a BSSE-corrected ΔE_{ads} of -25.0 kcal/mol which is close to the present result for the faceted (010). Although no relevant data are available for completely OH-free anatase, DMMP adsorption on OH-free rutile (110) at room temperature is largely molecular [29,30]. If the same is true for anatase (010) then the present results suggest that dissociation under these conditions is kinetically limited. This is consistent with experimental results for partially-hydroxylated TiO_2 powder [31,32] which indicate that surface OH is directly involved in the decomposition of molecular DMMP, possibly *via* a nucleophilic attack on the P atom by

14

the O atom of a Ti-OH group, and that this can occur below room temperature. In the present interpretation the Ti-OH is necessary to overcome the kinetic barrier to decomposition.

4. Conclusions

This is, to our knowledge, the first computational study of the faceted anatase (010) (or, equivalently, (100)) surface either with or without an adsorbate. On the bare surfaces, similar relaxations occur for corresponding atoms with and without faceting. These consist mainly of inward (outward) displacements of Ti_{5c} (Ti_{6c}) atoms and outward displacements of O_{3c} atoms. Surface O_{2c} atoms displace mainly parallel to the surface. The energies and structures for molecular adsorption of DMMP are similar in either case and are also similar to those [42] for rutile (110) and anatase (101) surfaces. Adsorption occurs preferentially *via* a Ti_{5c}---O=P dative bond with evidence of C-H---O bonding between methoxy groups and O_{2c} atoms. The results indicate that molecular adsorption of DMMP on HSA TiO_2 powders, for which the anatase (010) surface is a major constituent, can be understood without necessarily taking account explicitly of the faceting. As a corollary, the results also suggest that data for molecular adsorption of DMMP on the easily-obtained rutile (110) surface should be transferable to the less common anatase (010) surface. However, this applies only to the pristine surfaces considered here which are free of defects and adsorbed OH. The situation may change when such imperfections are introduced.

A possible first step in the dissociative adsorption of DMMP on OH-free surfaces was defined on the basis of experimental data [29,30] for OH-free rutile (110) single-crystal surfaces. On the non-defective and OH-free surface the product consists of an O_{2c}-CH_3 bond at a Ti-O_{2c}-Ti site and a $(CH_3)(CH_3O)P(-O-)_2$ bridge between two Ti_{5c} sites. ΔE_{ads} for this process indicates that it is thermodynamically favored over molecular adsorption but to a degree that depends on faceting. Faceting exposes the more stable (011) (or, equivalently, (101)) surface and reduces the

15

magnitude of ΔE_{ads} for dissociative adsorption, shifting it toward the result obtained for the (011). Experiments on fully OH-free anatase (010) surfaces are needed in order to determine whether dissociation is kinetically accessible without the intervention of Ti-OH sites.

Acknowledgements

Table 1

Observed and calculated TiO_2 lattice parameters[a]

	rutile[b]		anatase[c]	
	expt.	calc.	expt.	calc.
a	4.5937	4.564	3.7845	3.781
c	2.9587	2.987	9.5143	9.536
u	0.30478	0.3060	0.20806	0.2063
Volume	62.435	62.224	136.268	136.355

[a] Experimental values are from neutron diffraction data, ref 46. The lattice constants (a, c) are in

Ångstroms, and u is a fraction of a lattice constant. The volume of the crystallographic unit cell

(which comprises two primitive cells in the case of anatase) is given in $Å^3$.

[b] The rutile Ti positions are at (0,0,0) and (½, ½, ½). The O positions are at ±(u, u, 0),

(-u+½, u+½, ½) and (u+½, -u+½, ½).

[c] The anatase Ti positions are at ((0, 0, 0), (½, ½, ½)) + ((0, 0, 0), (0, ½, ¼)). The O positions are

at ((0, 0, 0), (½, ½, ½)) + ((0, 0, u), (0, ½, u+¼), (½, 0, -u+¾), (½, ½, -u+½))

Table 2

Displacements, relative to the ideally-terminated surface, resulting from relaxation of the unfaceted anatase (010) surface[a]

	atom[b]	this work[c]	ref. 37[d]	ref. 22[e]
	Ti_{5c}	0.02; -0.15	0.04; -0.14	0.02; -0.16
Layer 1	$O_{\parallel}$	0.02; +0.18	0.04; +0.18	0.04; +0.18
	$O_{\perp}$	0.17; 0.00	0.16; -0.01	0.16; +0.02
	Ti_{6c}	0.00; +0.12	0.00; +0.11	0.01; +0.17
Layer 2	$O_{\parallel}$	0.00; +0.07	0.00; +0.07	0.01; +0.10
	$O_{\perp}$	0.12; -0.04	0.11; -0.03	0.13; -0.03

[a] All displacements are in Ångstroms. Values are given as $|\Delta x|$; Δz where Δx is the displacement in the [001] direction, and Δz is the displacement along the surface normal. A positive (negative) Δz is outward (inward). Layer 1 is the surface layer. For $O_{\perp}$, Δx is in a direction away from the "channel" (cf. Fig. 1). *The anatase (100) and (010) surfaces are isostructural*.

[b] $O_{\parallel}$ refers to the O atom bonded to three Ti atoms in the same plane which, at the surface, is an O_{3c} site. $O_{\perp}$ refers to the O atom with bonds to Ti in different planes which, at the surface, is an O_{2c} site. See Fig. 1.

[c] Unfaceted (4x1) 2-DPS model with six layers after geometry relaxation as described in the text.

[d] (100)-(1x1) 2-DPS model with eight layers relaxed in an RHF calculation with ECPs for Ti and O (see ref. 37).

[e] (100)-(1x1) 2-DPS with six Ti layers relaxed in a DFT calculation using Car-Parrinello molecular dynamics (see ref. 22).

Table 3

Displacements, relative to the ideally-terminated surface, resulting from relaxation of the faceted anatase (010) surface[a]

	Layer 1			Layer 2	
	6 Layers	12 Layers		6 Layers	12 Layers
atom[b]	$\Delta x; \Delta z$	$\Delta x; \Delta z$	atom[b]	$\Delta x; \Delta z$	$\Delta x; \Delta z$
Ti_{5c} (1)	-0.05; -0.08	-0.02; -0.10	Ti_{5c} (1)	+0.06; -0.25	0.00; -0.16
Ti_{5c} (2)	-0.01; -0.13	+0.02; -0.10	Ti_{5c} (2)	0.00; -0.11	0.00; -0.16
$O_{\parallel}$ (1)	-0.05; +0.25	-0.02; +0.23	Ti_{6c} (1)	+0.04; +0.08	+0.02; +0.15
$O_{\parallel}$ (2)	0.00; +0.21	+0.03; +0.23	Ti_{6c} (2)	-0.04; +0.17	-0.02; +0.15
$O_{\perp}$ (1)	+0.13; 0.00	+0.16; +0.04	$O_{\parallel}$ (1)	+0.05; +0.09	+0.01; +0.20
$O_{\perp}$ (2)	-0.19; +0.05	-0.16; +0.04	$O_{\parallel}$ (2)	-0.02; +0.25	-0.01; +0.20
			$O_{\parallel}$ (3)	+0.08; 0.00	+0.04; +0.06
			$O_{\parallel}$ (4)	-0.05; +0.07	-0.04; +0.06
			$O_{\perp}$ (1)	+0.24; +0.01	+0.19; -0.02
			$O_{\perp}$ (2)	-0.19; 0.01	-0.18; -0.01
			$O_{\perp}$ (3)	+0.13; +0.01	+0.12; +0.01
			$O_{\perp}$ (4)	-0.14; -0.01	-0.12; +0.01

[a] See Table 2, footnote a. "6 Layers" refers to the 2-DPS with a (4x2) supercell and 6 layers (before introduction of the facet). "12 Layers" refers to the 2-DPS with a (1x2) supercell and 12 layers (before faceting). See Sec. 3.1 for further details.

[b] See Table 2, footnote b, and Fig. 2.

References

[1] U. Diebold, Surf. Sci. Rep. 48 (2003) 53.

[2] A. Fujishima, X. Zhang, D.A. Tryk, Surf. Sci. Rep. 63 (2008) 515.

[3] G. Spoto, C. Morterra, L. Marchese, L. Orio, A. Zecchina, Vacuum 41 (1990) 37.

[4] G. Cerrato, L. Marchese, C. Morterra, Appl. Surf. Sci. 70/71 (1993) 200.

[5] G. Martra, Appl. Catal. A: General 200 (2000) 275.

[6] A. Feldhof, C. Mendive, T. Bredow, D. Bahnemann, Chem. Phys. Chem. 8 (2007) 805.

[7] P. Wen, H. Itoh, W. Tang, Q. Feng, Langmuir 23 (2007) 11782.

[8] S. Dzwigaj, C. Arrouvel, M. Breysse, C. Geantet, S. Inoue, H. Toulhoat and P. Raybaud, J. Catal. 236 (2005) 245.

[9] B. Mguig, M. Calatayud, C. Minot, Surf. Rev. Lett. 10 (2003) 175.

[10] M. Calatayud and C. Minot, Surf. Sci. 552 (2004) 169.

[11] A. Bouzoubaa, A. Markovits, M. Calatayud, C. Minot, Surf. Sci. 583 (2005) 107.

[12] T. Homann, T. Bredow, K. Jug, Surf. Sci. 555 (2004) 135.

[13] V.P. Indrakanti, J.D. Kubicki, H.H. Schobert, Energy and Fuels 22 (2008) 2611.

[14] H.S. Wahab, T. Bredow, S.M. Aliwi, J. Mol. Struct: THEOCHEM 868 (2008) 101.

[15] H. S. Wahab, T. Bredow, S.M. Aliwi, Chem. Phys. 353 (2008) 93.

[16] H.S. Wahab, T. Bredow, S.M. Aliwi, Surf. Sci. 603 (2009) 664.

[17] H. Kusama, H. Orita, H. Sugihara, Langmuir 24 (2008) 4411.

[18] G. Capecchi, M.G. Faga, G. Martra, S. Coluccia, M.F. Iozzi, M. Cossi, Res. Chem. Intermed. 33 (2007) 269.

[19] C.B. Mendive, T. Bredow, A. Feldhoff, M.A. Blesa, D. Bahnemann, Phys. Chem. Chem. Phys. 11 (2009) 1794.

[20] C. Arrouvel, M. Digne, M. Breysse, H. Toulhoat and P. Raybaud, J. Catal. 222 (2004) 152.

[21] C. Arrouvel, M. Toulhoat, M. Breysse, and P. Raybaud, J. Catal. 226 (2004) 260.

[22] M. Lazzeri, A. Vittadini and A. Selloni, Phys. Rev. B 63 (2001) 155409; Erratum, *ibid.* 65 (2002) 119901.

[23] N. Ruzycki, G.S. Herman, L.A. Boatner, U. Diebold, Surf. Sci. 529 (2003) L239.

[24] S. Han, G. Zhang, H. Xi, D. Xu, X. Fu, X. Wang, Catal. Lett. 122 (2008) 106.

[25] A. Kiselev, A. Mattson, M. Andersson, A.E.C. Palmqvist, L. Österlund, J. Photochem. Photobiol. A: Chem. 184 (2006) 125.

[26] D.A. Trubitsyn, A.V. Vorontsov, J. Phys. Chem. B 109 (2005) 21884.

[27] D.A. Panayotov, J.R. Morris, J. Phys. Chem. C 112 (2008) 7496.

[28] J.S. Ratliff, S.A. Tenney, X. Hu, S.F. Conner, S. Ma, D.A. Chen, Langmuir 25 (2009) 216.

[29] J. Zhou, S. Ma, Y.C. Kang, D.A. Chen, J. Phys. Chem. B 108 (2004) 11633.

[30] J. Zhou, K. Varazo, J.E. Reddic, M.L. Myrick, D.A. Chen, Anal. Chim. Acta 496 (2003) 289.

[31] C.N. Rusu, J.T. Yates, Jr., J. Phys. Chem. B 104 (2000) 12292.

[32] D.A. Panayotov, J.R. Morris, Langmuir 25 (2009) 3652.

[33] R. Dovesi, V.R. Saunders, C. Roetti, R. Orlando, C.M. Zicovich-Wilson, F. Pascale, B. Civalleri, K. Doll, N.M. Harrison, I.J. Bush, Ph. D'Arco, M. Llunell, CRYSTAL 06 User's Manual 2007, Theoretical Chemistry Group, University of Turin. The manual and basis sets may be obtained at http://www.crystal.unito.it/

[34] C. Pisani, R. Dovesi, C. Roetti, Hartree-Fock Ab-Initio Treatment of Crystalline Systems, Lecture Notes in Chemistry, Vol. 48, Springer, Berlin, 1988.

[35] C. Pisani, Quantum-Mechanical Ab-Initio Calculation of the Properties of Crystalline Materials, Lecture Notes in Chemistry, Vol. 67, Springer, Berlin, 1996.

[36] V. Swamy, J. Muscat, J.D. Gale, N.M. Harrison, Surf. Sci. 504 (2002) 115.

[37] F. Labat, P. Baranek, C. Adamo, J. Chem. Theory Comput. 4 (2008) 341.

[38] M. Levy, J.P. Perdew, J. Chem. Phys. 84 (1986) 4519.

[39] S. Piskunov, E. Heifets, R.I. Eglitis, G. Borstel, Comput. Mater. Sci. 29 (2004) 165. The Ti ECP basis set from this reference, as given at the *CRYSTAL 06* website [33], contains a very minor typographical error. The second *s* coefficient of the inner-most *sp* shell is given in the original reference as 0.348881629.

[40] K.L. Schuchardt, B.T. Didier, T. Elsethagen, L. Sun, V. Gurumoorthi, J. Chase, J. Li, T.L. Windus, J. Chem. Inf. Model. 47 (2007) 1045.

[41] F. Labat, P. Baranek, C. Domain, C. Minot, C. Adamo, J. Chem. Phys. 126 (2007) 154703.

[42] V.M. Bermudez, J. Phys. Chem. C - in press.

[43] C. Zhang, P. J. D. Lindan, J. Chem. Phys. 118 (2003) 4620.

[44] R.D. Suenram, F.J. Lovas, D.F. Plusquellic, A. Lesarri, Y. Kawashima, J.O. Jensen, A.C. Samuels, J. Mol. Spectrosc. 211 (2002) 110.

[45] A. Cuisset, G. Mouret, O. Pirali, P. Roy, F. Cazier, H. Nouali, J. Demaison, J. Phys. Chem. B 112 (2008) 12516.

[46] C.J. Howard, T.M. Sabine and F. Dickson, Acta Cryst. B47 (1991) 462.

[47] G.R. Desiraju, Acc. Chem. Res. 29 (1996) 441.

[48] J. Scaranto, S. Giorgianni, J. Mol Struct.: THEOCHEM 858 (2008) 72.

[49] H. Perron, J. Vandenborre, C. Domain, R. Drot, J. Roques, E. Simoni, J.-J. Ehrhardt, H. Catalette, Surf. Sci. 601 (2007) 518.

[50] P.M. Kowalski, B. Meyer, D. Marx, Phys. Rev. B 79 (2009) 115410.

[51] R.F.W. Bader, Atoms in Molecules: A Quantum Theory, Clarendon, Oxford, 1990.
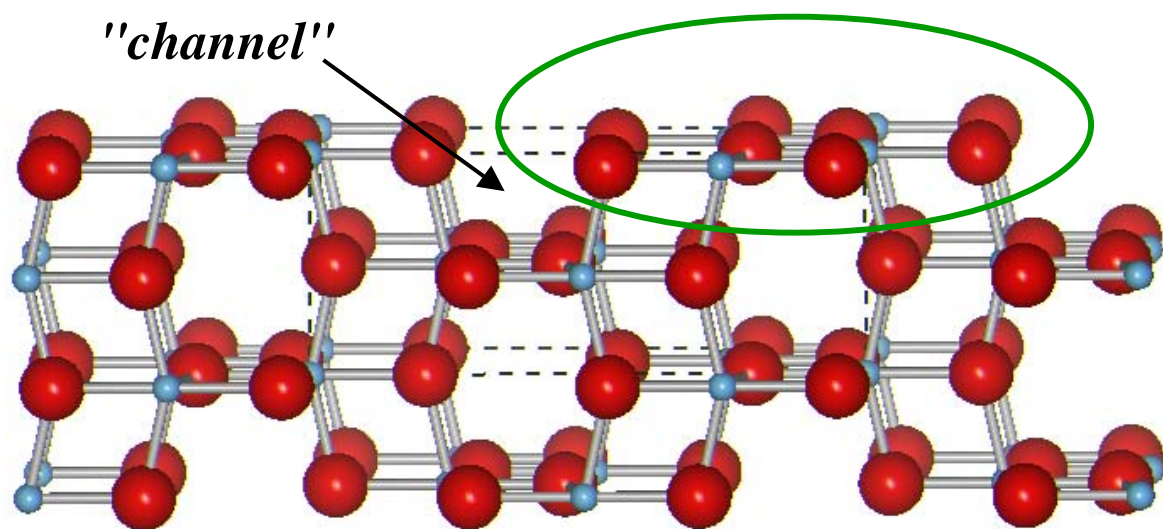
Figure captions

Fig. 1   The anatase (010) surface with the bulk unit cell shown by the dashed lines. Blue (red) spheres are Ti (O). (a) Shows the ideally-terminated surface, and (b) shows a (1x2) faceted structure (ref. 23). Both structures are shown before relaxation. The different models are not to scale. The encircled section in (a) shows what is removed in forming the facet. Various surface sites are labeled (see text), and the region referred to as the "channel" in the text is indicated. The plane shown in (b) is the (011), which is isostructural with the (101).

Fig. 2   The faceted surface after relaxation. In correspondence to Table 2, the brackets indicate the layer numbers, and the individual atoms are labeled by type. For clarity, Ti (O) atoms are labeled on the "top" ("bottom") of the slab. The Layer 1 $Ti_{5c}(2)$ is obscured by an O atom. The Layer 2 Ti_{5c} site shown italicized in blue is the one used for DMMP adsorption within the facet (see text). The [001] and [010] vectors define the positive directions for Δx and Δz, respectively, for the "top" surface atoms (cf. Table 2 and discussion in text). The [001] and [010] directions are reversed on the "bottom" surface
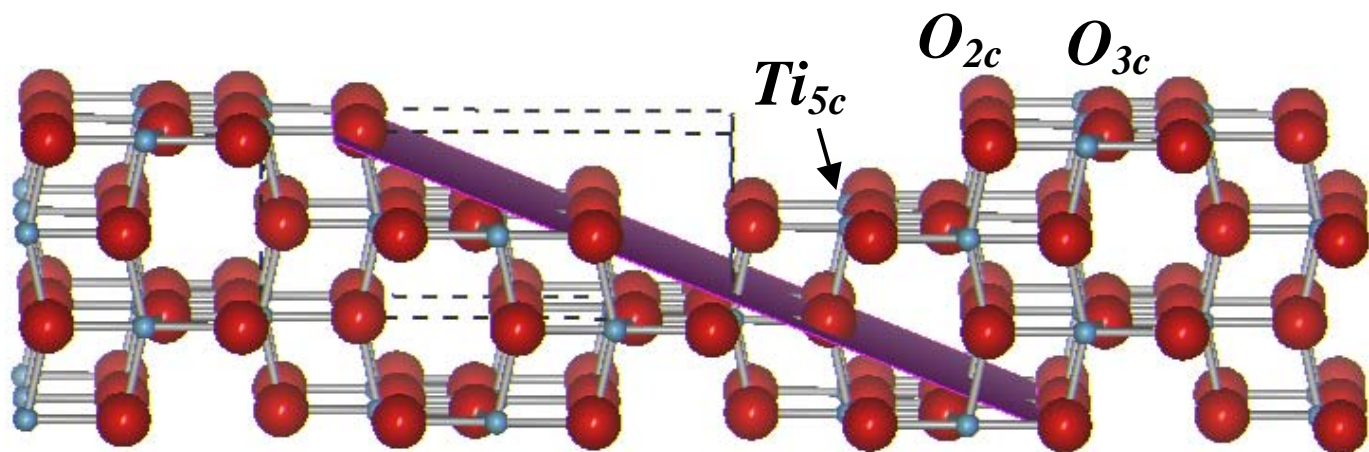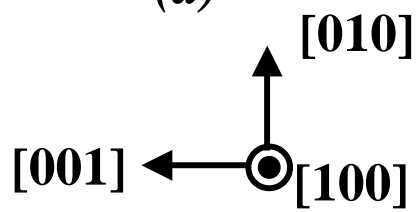
Fig. 3   Sections of the (a) unfaceted and (b) faceted surface after relaxation with adsorbed DMMP in the lowest-energy conformations. For clarity, only sections of the entire slab supercells are shown. The dashed lines show H-bonding interactions identified as such on the basis of the O_{2c}---H and O_{2c}---C distances and the O_{2c}---H-C angle (see text). In (b) the adsorption site is the one designated Layer 2 $Ti_{5c}(1)$ in Fig. 2. Note that the orientation in (b) is reversed relative to that in Fig. 2. The green, black and gray spheres represent P, C and H respectively.

Fig. 4   Similar to Fig. 3 but showing structures considered for the first step in DMMP dissociation. The upper panel shows the unfaceted surface viewed along the (a) [100] and (b) [001] direction. (c) Shows the faceted surface viewed along the [100] direction. Possible H-bonding in-

teractions have been omitted for clarity. The arrow in Fig. 4b marks an alternative location for
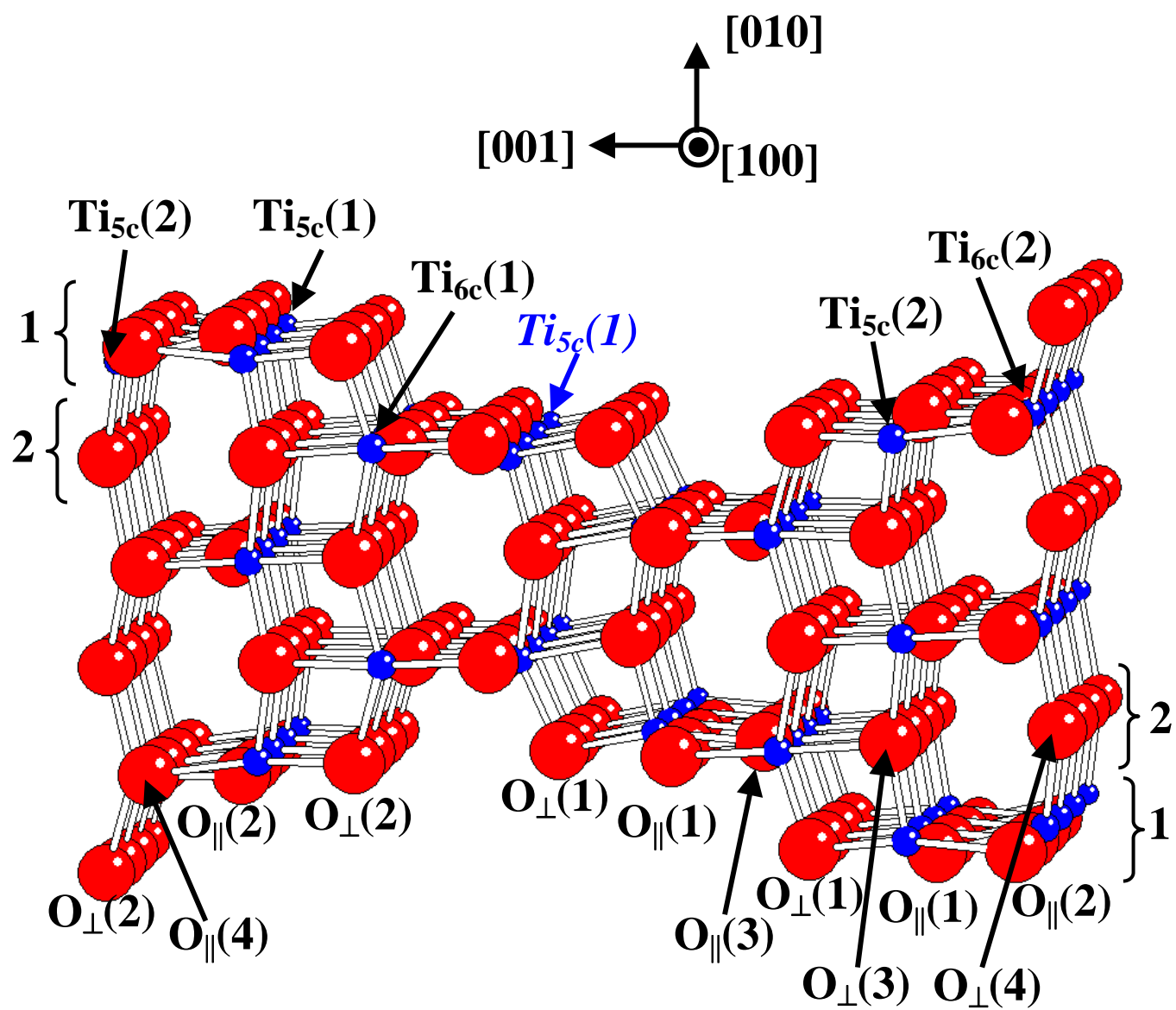
the CH_3 fragment which is discussed in Sec. 3.3.

"channel"

(a)
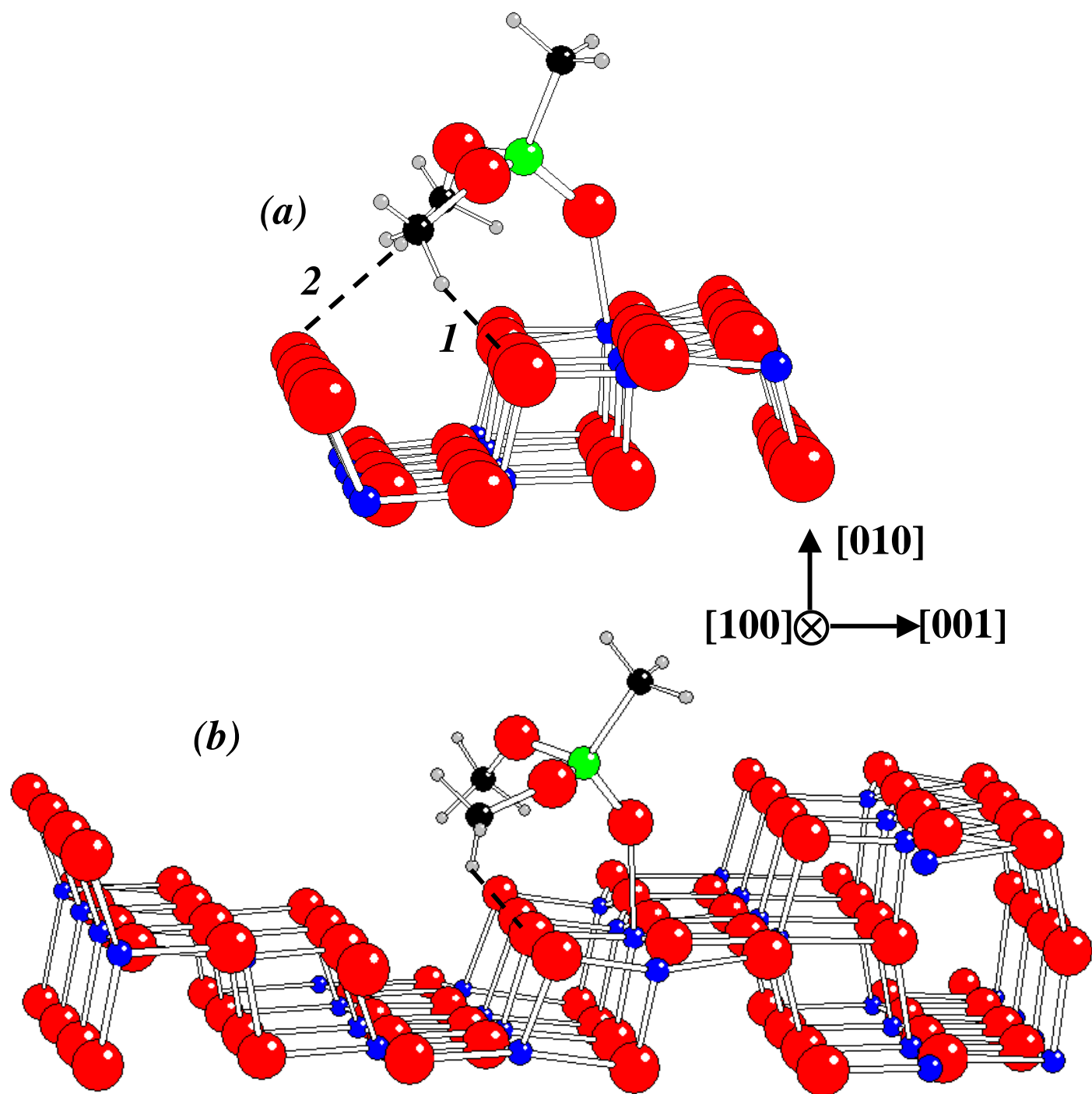
[010]
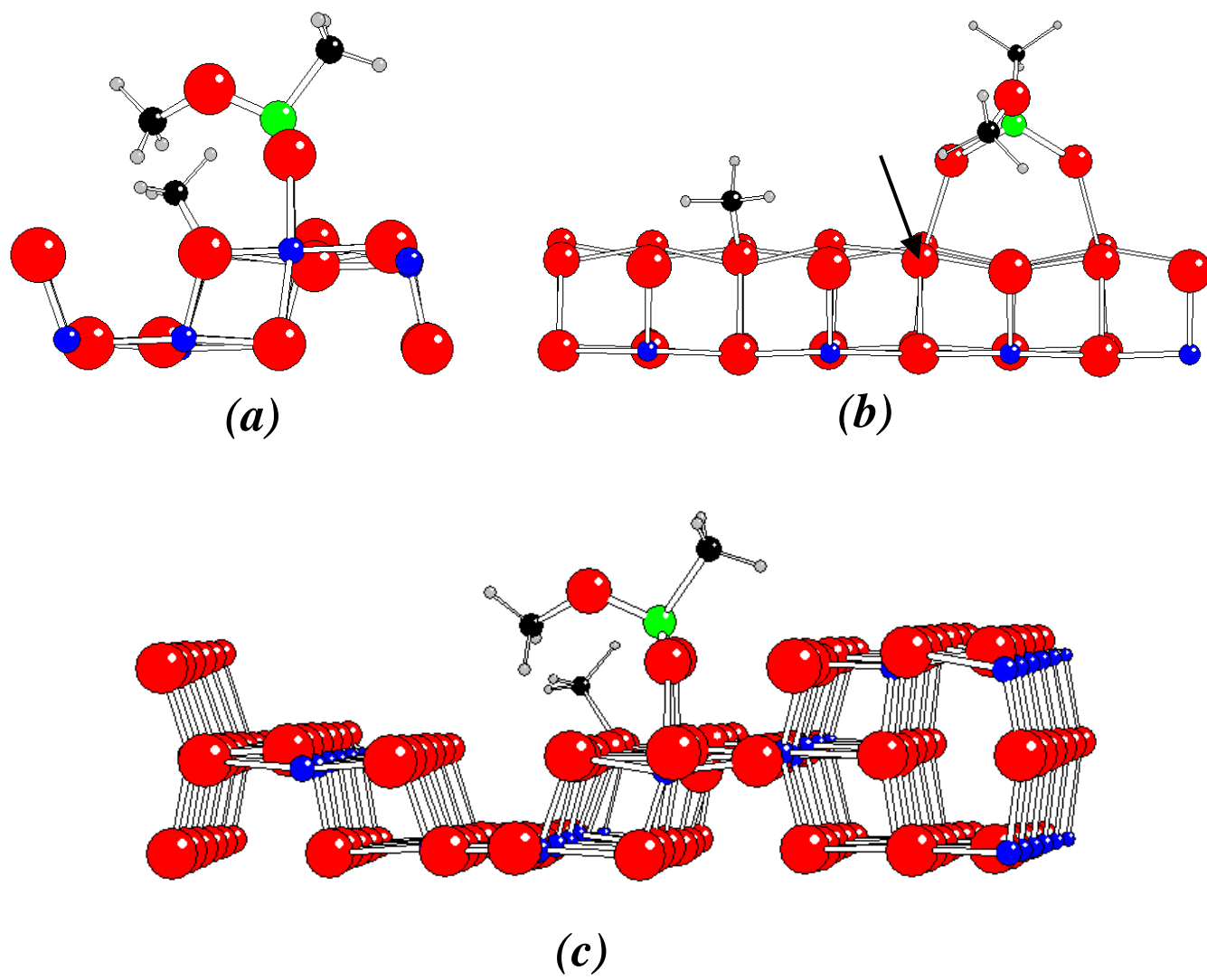
[001] ⊙ [100]

Ti_{5c} O_{2c} O_{3c}

(b)

Fig. 1

Fig. 2

(a)

2

1

[010]

[100]⊗ → [001]

(b)

Fig. 3

(a)

(b)

(c)

Fig. 4